International Journal of Management, IT & Engineering
Vol. 8 Issue 2, February 2018,
ISSN: 2249-0558 Impact Factor: 7.119
Journal Homepage: http://www.ijmra.us, Email: editorijmie@gmail.com
Double-Blind Peer Reviewed Refereed Open Access International Journal - Included in the International Serial Directories Indexed & Listed at: Ulrich's Periodicals Directory ©, U.S.A., Open J-Gate as well as in Cabell's Directories of Publishing Opportunities, U.S.A

STUDY OF $Nd_{1.65}Sr_{0.35}NiO_{4+\delta}$ CATHODE MATERIAL FOR INTERMEDIATE TEMPERATURE SOLID OXIDE FUEL CELL

J. D. PUNDE
Department of Physics, S. S. Girls' College, Gondia - 441 601, India.

Abstract

The $Nd_{1.65}Sr_{0.35}NiO_{4+\delta}$ were prepared by combustion technique. It is mixed ionic - electronic conducting (MIEC) oxides and has K_2NiF_4 - type A_2BO_4 structure. The prepared samples were characterized using X -ray powder diffraction (XRD), Fourier Transformation Infrared Spectroscopy (FTIR), micro-hardness testing and four-probe dc conductivity. A close scrutiny of XRD reveals that the prepared solid solutions of cathode are single-phase and the *d* -values matches well with the standard JCPDS data corresponding to pure Nd_2NiO_4 with small deviation, FTIR spectra shows the prepared sample have K_2NiO_4 - type structure and the transition from negative temperature coefficient to positive temperature coefficient, within the solid solubility region, is observed at 931 K in dc conductivity data.

Keywords: Intermediate temperature solid oxide fuel cell (IT-SOFC), mixed ionic-electronic conductor (MIEC), K_2NiF_4, combustion method,cathode.

Introduction

Consumption of energy is a fundamental requirement of modern world to improve the life style along with increase in population. The majority of energy required worldwide is generated from the combustion of fossil fuels. Although these resources are essential to the world, combustion of fossil fuels has resulted in increased health risks and global warming. Solar panels and wind farms are familiar alternative energy generation technology to fossil fuel. Besides, they also have some limitations such as: On cloudy days and at night, solar

panels are unable to generate energy. Similar is the case with wind farms on windless day [1]. Furthermore, these sources are less efficient and non-portable. Solid oxide fuel cells (SOFCs) have potential to fulfill all these requirements.

Solid Oxide Fuel Cells (SOFCs) are electrochemical devices that produce electricity and heat directly from gaseous fuels through an oxidation process with high efficiency and low pollution [2]. But the technological development of SOFCs is limited due to their high operating temperatures, typically around$800℃ - 1000℃$. In this temperature range, low-cost interconnect materials are not useful, and long-term stability of the cell cannot be ensured as chemical reactions occur between electrodes and electrolyte [3]. In recent years, great efforts are directed to develop intermediate temperature SOFCs (IT-SOFCs) operating in the range $500℃ - 800℃$. Lowering operating temperature can suppress degradation of components and extend the range of acceptable materials selection; this, also, improves cell durability and reduces the system cost. For the furtherimprovement of the IT-SOFCs performance, the development ofhigh-performance cathode material is critical.Potential cathode materials must exhibit electronic as well as oxygen ion-conductivity to increase the electrochemical reaction sites. Consequently, the mixed-ionic-electronic conductors (MIECs) have currently attracted a great deal of attention.

The MIECs with K_2NiF_4-type oxides structureexhibit anisotropic electrical transport property due to their specific crystallographic characters. The structure of K_2NiF_4-type oxides, as an example ofA_2BO_4(A-rare earth, alkaline-earth; B-transition metal),consists of the stacking of perovskite ABO_3 layers alternating with rock salt AO layers along the c-direction [4]. A_2BO_4compounds exhibit high electronic conductivity. Also, possibility of forming solid solutions with mixed valence of the B-site provides good scope to tailor the physical-chemical properties. In addition, a high concentration of oxygen interstitials offers rapid oxygen transport through crystal, eventually a scope for developing a new type of MIEC cathode materials [5].

In this study, the MIEC$Nd_{1.65}Sr_{0.35}NiO_{4+\delta}$was prepared by combustion technique. The prepared samples were characterized using X-ray powder diffraction (XRD), micro-hardness testing, Fourier Transform Infrared Spectroscopy (FTIR)and four-probe dc conductivity.

International Journal of Management, IT & Engineering
Vol. 8 Issue 2, February 2018,
ISSN: 2249-0558 Impact Factor: 7.119
Journal Homepage: http://www.ijmra.us, Email: editorijmie@gmail.com
Double-Blind Peer Reviewed Refereed Open Access International Journal - Included in the International Serial Directories Indexed & Listed at: Ulrich's Periodicals Directory ©, U.S.A., Open J-Gate as well as in Cabell's Directories of Publishing Opportunities, U.S.A

Experimental

The initial reagents neodymium acetate, strontium acetate and nickel acetate, used were procured from Aldrich Chemicals (USA) with purity > 99.9 %. All these reagents were dried at 393 K for 24 h in order to remove the traces of moisture present. The respective requisite reagents in stoichiometric ratio were dissolved in the double distilled deionised water separately and then mixed together in a single corning flask. The homogeneous aqueous solution was then heated by using hot plate. The residue obtained was then pulverized to get them in the form of powders. The pellets of diameter and thickness 13mm and 1-2 mm, respectively, were obtained by uniaxially compressing ground powder at 3 tonscm^{-2} pressure with the help of Specac (UK) stainless steel die-punch and hydraulic press. The resulting pellets were initially calcined at 973 K for 4 h in an electric furnace. Subsequently, they were crushed to obtained fine powder and re-pelletized of diameter and thickness 9 mmand 1-2 mm, respectively. The pellets were finally sintered at 1273 K for 4 h and allowed to cool in the furnace to room temperature.

The prepared sample was subjected to structural characterization by X-ray powder diffraction (XRD) with a PANalyticalX'pert PRO (Philips, the Netherlands) instrument that employed CuK_α radiation. A curved graphite crystal was used as a monochromator. The X-ray diffraction measurement were carried out in a 2Θ range from 10 to 80° with a step size and time per step of 0.020° and 5 s, respectively. The IR spectra were recorded by ECO-ATR Fourier transform instrument. The spectra of powder sample were recorded in the region 4000 - 600 cm^{-1}. The sintered densities of the sample was determined using Archimedes' principle with the help of Mettler XS105 dual range monopan balance with density kit attachment and built in density measurement software. The micro-hardness of the sample was measured by the Vickers indentation technique (HMV2 Series Shimadzu micro Hardness Tester, Japan).

A thin platinum film on both flat surfaces of the sintered pellet was obtained by d.c. sputtering and resulted in good ohmic contacts for d.c. electrical conductivity measurements. Prior to the conductivity measurement, the sample was spring-loaded in a ceramic cell holder (Amel, Italy) and heated to 973 K for 1 h to homogenize the charge carriers. The resistance

during the cooling cycle was measured as a function of temperature using the four-probe method with a computer-controlled Keithley 6221 current source and a 2182A nanovoltmeter in delta mode. The temperature of the sample during the measurement was controlled with an accuracy of ±1 K with a Eurotherm 2216e temperature controller. The tip of a calibrated thermocouple was kept in the vicinity of the sample to measure its actual temperature.

Result and discussion

X-ray powder diffraction

The X-ray powder diffraction (XRD) patterns of $Nd_{1.65}Sr_{0.35}NiO_{4+\delta}$ is shown in the Fig. 1. All the diffracted lines are broader than usually observed for good crystalline solids. The broadening of diffracted lines is attributed to the superfine crystallite nature of material. A careful look at the Fig. 1 revealed close matching of all the characteristic diffracted lines with the JCPDS (joint committee for powder diffraction standard) data (File No. 01-080-2323) corresponding to pure tetragonal Nd_2NiO_4. Absence of diffracted line corresponding to either reagents or any intermediate compound confirmed the formation of single-phase tetragonal $Nd_{1.65}Sr_{0.35}NiO_{4+\delta}$solid solution. In order to ascertain the formation of solid solution and its consequence on host lattice structure, the lattice cell constants of the samples under study were determined using Unitcell, a computer software [6]. The lattice constant *a* matched well with the values *a* = 0.3809 nm (of Nd_2NiO_4) reported in literature [7,8] but the value of lattice constant *c* increase. Since the ionic radii of Nd^{3+} is (11.63 nm) smaller than that of Sr^{2+} (13.1 nm) [9], partial replacement of former by latter resulted in lattice expansion of host Nd_2NiO_4. The lattice distortion along *c*-axis due to partial replacement of host by smaller cation in K_2NiF_4-type lattice has been reported in literature [10, 11].

International Journal of Management, IT & Engineering
Vol. 8 Issue 2, February 2018,
ISSN: 2249-0558 Impact Factor: 7.119
Journal Homepage: http://www.ijmra.us, Email: editorijmie@gmail.com
Double-Blind Peer Reviewed Refereed Open Access International Journal - Included in the International Serial Directories Indexed & Listed at: Ulrich's Periodicals Directory ©, U.S.A., Open J-Gate as well as in Cabell's Directories of Publishing Opportunities, U.S.A

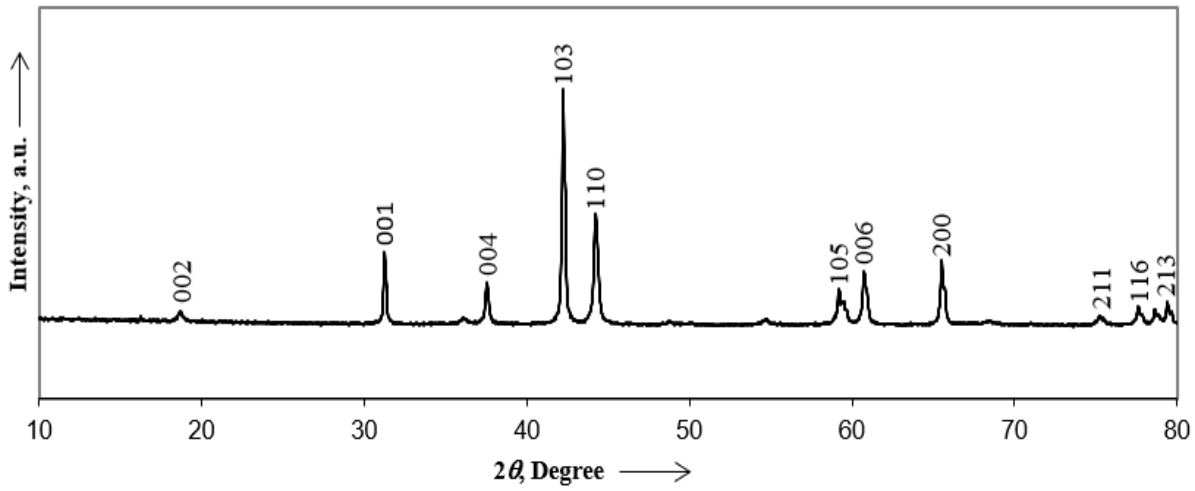

Fig. 1: The XRD patterns of $Nd_{1.65}Sr_{0.35}NiO_{4+\delta}$

Table 1: A lattice cell constants (a, c and v), crystallite size (C_s), crystal lattice strain (S_l), sinter density (ρ) and microhardness number (HV) of $Nd_{1.65}Sr_{0.35}NiO_{4+\delta}$.

Composition	*a* (*nm*)	*c* (*nm*)	*v* (nm^3)	C_s (*nm*)	S_l (%)	ρ (%)	HV
JCPDS	0.3854	1.214	--	-	--	-	--
$Nd_{1.65}Sr_{0.35}NiO_{4+\delta}$	0.381	1.240	0.163	242.5	0.13	81.5	201

The crystallite size of composition under study is 242.5 determined using X'pertHighscore plus software based on the following expression:

$$C_s = \frac{0.9\lambda}{\beta \cos\theta_B}, \qquad (1)$$

where C_s,λ, and θ_B are thickness of crystallite, X-ray wavelength and Bragg's angle, respectively. Here, β was determined by:

International Journal of Management, IT & Engineering
Vol. 8 Issue 2, February 2018,
ISSN: 2249-0558 Impact Factor: 7.119
Journal Homepage: http://www.ijmra.us, Email: editorijmie@gmail.com
Double-Blind Peer Reviewed Refereed Open Access International Journal - Included in the International Serial Directories Indexed & Listed at: Ulrich's Periodicals Directory ©, U.S.A., Open J-Gate as well as in Cabell's Directories of Publishing Opportunities, U.S.A

$$\beta^2 = \beta_m^2 - \beta_s^2, \qquad (2)$$

where, β_m and β_s were the measured and the standard full width of half maxima, FWHM, of diffracted line, respectively. The β_s was estimated from the XRD pattern obtained by running the experiment on a standard silicon sample provided by PANalytical, Netherlands.

Sinter density and microhardness number

The sintered density (ρ) of the $Nd_{1.65}Sr_{0.35}NiO_{4+\delta}$determined using the Archimedes principle, is given in Table 1. A close look at the table reveals that the sintered density$Nd_{1.65}Sr_{0.35}NiO_{4+\delta}$is comparable to $Nd_{1.7}Sr_{0.3}NiO_{4+\delta}$and $Nd_{1.6}Sr_{0.4}NiO_{4+\delta}$reported in the same study [12]. The hardness number (*HV*)of $Nd_{1.65}Sr_{0.35}NiO_{4+\delta}$ is less than $Nd_{1.8}Sr_{0.2}NiO_{4+\delta}$ and greater than $Nd_{1.6}Sr_{0.4}NiO_{4+\delta}$ [13]. The sinter density and microhardness number of the sample under study is close match the with the previously reported data.

Fourier Transform Infrared Spectroscopy (FTIR)

Fourier Transform Infrared Spectroscopy (FTIR) spectra of $Nd_{1.65}Sr_{0.35}NiO_{4+\delta}$ in the region 4000 - 400 $cm^{-1}$is shown in Fig. 2. A close look at the figures reveals presence of broad absorption peaks in the region 3500-2200 cm^{-1} for the given sample. The absorption band at the region 700-600 $cm^{-1}$and 500-400 cm^{-1}prove the material have K_2NiF_4 -type A_2BO_4 structure [14, 15]. The FTIR spectra of the sample of mixed oxides show weak absorption at 700–400cm^{-1}, which indicates that the $Nd_{1.65}Sr_{0.35}NiO_{4+\delta}$ structure becomesmicrostrained and the microstrainof the coordination polyhedra depends on Ni. A low microstrain density does not change the original structure [16].

International Journal of Management, IT & Engineering
Vol. 8 Issue 2, February 2018,
ISSN: 2249-0558 Impact Factor: 7.119
Journal Homepage: http://www.ijmra.us, Email: editorijmie@gmail.com
Double-Blind Peer Reviewed Refereed Open Access International Journal - Included in the International Serial Directories Indexed & Listed at: Ulrich's Periodicals Directory ©, U.S.A., Open J-Gate as well as in Cabell's Directories of Publishing Opportunities, U.S.A

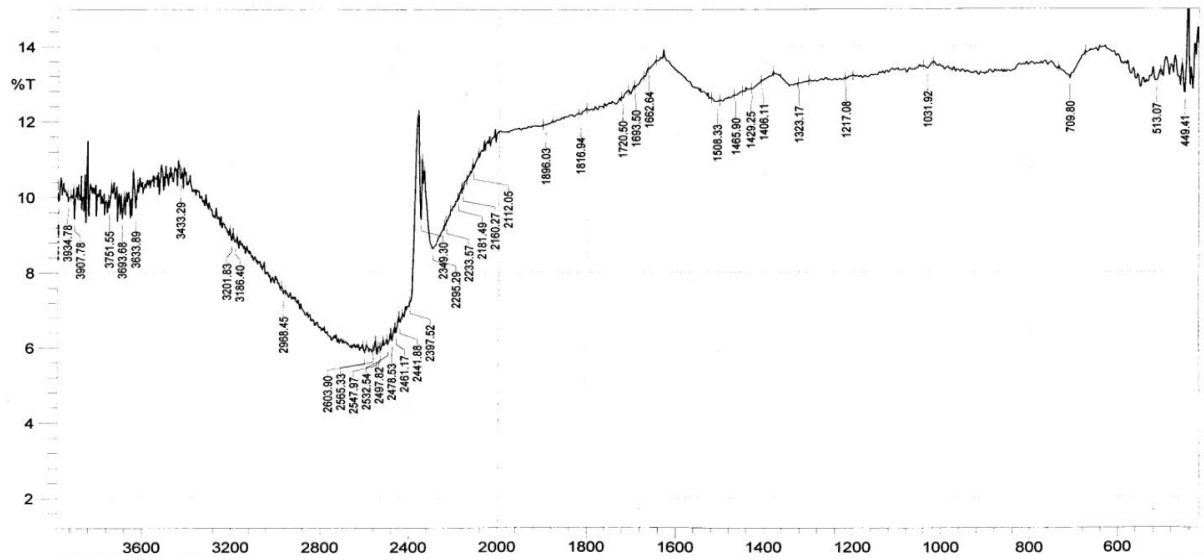

Fig. 2: FTIR spectra of $Nd_{1.65}Sr_{0.35}NiO_{4+\delta}$

dc conductivity

The variation of dc conductivity with temperature of the $Nd_{1.65}Sr_{0.35}NiO_{4+\delta}$ under study is shown in Fig. 3. As seen, the $Nd_{1.65}Sr_{0.35}NiO_{4+\delta}$ exhibited PTC, positive temperature coefficient, to NTC, negative temperature coefficient, transition in conductivity at about 913 *K*. Such transition has been better explained by the defect chemistry [17]. As a matter of fact, the electron holes ($h^{\bullet}$) conductivity is proportional to their charge *e*, concentration c_p and mobility μ_p according to expression given below:

$$\sigma_p = ec_p\mu_p. \quad (3)$$

Intrinsically, electrons and holes can be produced in Nd_2NiO_4 lattice by the following two-point defect equilibria:

$$O_O \Leftrightarrow V_O^{\bullet\bullet} + 2e' + \tfrac{1}{2}O_2, \quad (4)$$

$$\tfrac{1}{2}O_2 \Leftrightarrow O_i'' + 2h^{\bullet}, \quad (5)$$

coupled with intrinsic ionization

$$nil \Leftrightarrow e' + h^{\bullet}. \quad (6)$$

International Journal of Management, IT & Engineering
Vol. 8 Issue 2, February 2018,
ISSN: 2249-0558 Impact Factor: 7.119
Journal Homepage: http://www.ijmra.us, Email: editorijmie@gmail.com
Double-Blind Peer Reviewed Refereed Open Access International Journal - Included in the International Serial Directories Indexed & Listed at: Ulrich's Periodicals Directory ©, U.S.A., Open J-Gate as well as in Cabell's Directories of Publishing Opportunities, U.S.A

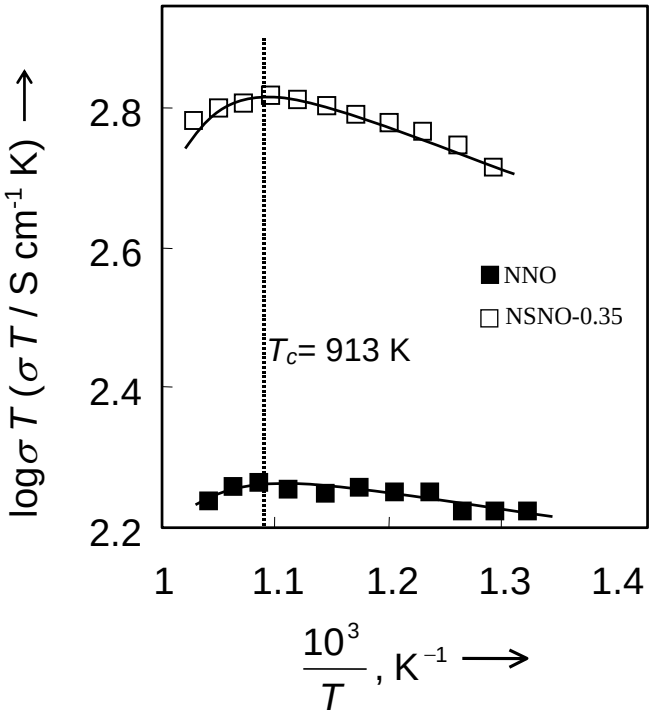

Fig. 3: Arrhenius plots for $Nd_{1.65}Sr_{0.35}NiO_{4+\delta}$

At temperature lower than 913 K, the chemical composition was almost steady; and so all the samples exhibited semiconducting behavior obeying the Arrhenius law, *i.e.*,

$$\sigma T = (\sigma T)_0 \exp\left(\frac{-E_a}{kT}\right), \qquad (7)$$

where $(\sigma T)_0$,k, T and E_a are pre-exponential factor, Boltzmann constant, absolute temperature and activation energy, respectively. At higher temperatures (> 913 K), however, $Nd_{1.65}Sr_{0.35}NiO_{4+\delta}$ solid solutions lose some oxygen according to reaction (Eq.5) [18]. Concurrently, correlatively decreased charge holes carrier density (c_p) that eventually reduced the dc conductivity (Fig. 3) above 913 K. There were no dc conductivity data/results reported in the literature on this system for a comparison.

International Journal of Management, IT & Engineering
Vol. 8 Issue 2, February 2018,
ISSN: 2249-0558 Impact Factor: 7.119
Journal Homepage: http://www.ijmra.us, Email: editorijmie@gmail.com
Double-Blind Peer Reviewed Refereed Open Access International Journal - Included in the International Serial Directories Indexed & Listed at: Ulrich's Periodicals Directory ©, U.S.A., Open J-Gate as well as in Cabell's Directories of Publishing Opportunities, U.S.A

In $Nd_{1.65}Sr_{0.35}NiO_{4+\delta}$, Sr^{2+} goes to the neodymium sites $\left(Sr'_{Nd}\right)$ with one effective negative charge, interstitial oxygen ions $\left(O''_i\right)$ with double negative effective charge; and Ni^{3+} on regular lattice site with one effective positive charge $\left(Ni^{\bullet}_{Ni}\right)$ [18]. The partial substitution of Sr^{2+} for Nd^{3+}, thus, introduced extrinsic defects according to quasi-chemical reaction:

$$2Ni^{x}_{Ni} + \tfrac{1}{2}O_2 \Leftrightarrow 2Ni^{\bullet}_{Ni} + O''_i, \qquad (8)$$

where, Ni^{x}_{Ni} are the Ni^{2+} and $Ni^{\bullet}_{Ni}$ the Ni^{3+}. Alternatively, for $Nd_{1.65}Sr_{0.35}NiO_{4+\delta}$ with $\delta>0$, the electroneutrality condition can be written as:

$$2\left[O''_i\right] + \left[Sr'_{Nd}\right] = \left[Ni^{\bullet}_{Ni}\right] = \left[h^{\bullet}\right] \qquad (9)$$

The corresponding defect equilibrium can be written as:

$$\frac{1}{2}O_2 + V_i^{x} \Leftrightarrow O''_i + 2h^{\bullet} \qquad (10)$$

Thus, the charge carrier density increases with an increasing oxygen concentration and the conductivity as per relation (3).

Conclusions

The $Nd_{1.65}Sr_{0.35}NiO_{4+\delta}$ solid solution prepared by combustion synthesis.XRD confirms the formation of single phase $Nd_{1.65}Sr_{0.35}NiO_{4+\delta}$. It is crystallizing with the tetragonal K_2NiF_4- type structure.The FTIR study indicates that the $Nd_{1.65}Sr_{0.35}NiO_{4+\delta}$ structure becomesmicrostrained and the microstrain of the coordination polyhedra depends on Ni. Temperature dependent σ exhibits PTC to NTC transition at 931 K. Since the doped $NdNiO_4$ less attended as cathode for IT-SOFC therefore,$Nd_{1.65}Sr_{0.35}NiO_{4+\delta}$may be potential candidate for IT-SOFC cathode.

Acknowledgements

The authors are thankful to Materials Science Research Laboratory, Department of Physics, RTM, Nagpur University, Nagpur.

References:

1. E. J. De. Guire, solid oxide fuel cells, review article (2003) http://www.csa.com/discoveryguides/fuecel/overview.php.
2. Assessment of finite volume modeling approaches for intermediate temperature Solid Oxide Fuel Cells working with CO-rich syngas fuels, V. Spallinaa, L. Mastropasqua b, P. Iora c, M.C. Romano b, S. Campanari b, international journal of hydrogen energy 40 (2015) 1501 2e15031.
3. F. Mauvy, J.-M. Bassat, E. Boehm, J.-P. Manaud, P. Dordor, J.-C. Grenier, *Solid State Ionics* 17– 28 (2003) 158.
4. E. N. Naumovich, M. V. Patrakeev, V. V. Kharton, A. A. Yaremechenko, D. I. Logvinovich, F. M. B. Marques, *Solid State Sci.* 7 (2005) 1353/ H. Zhao, Q. Li, L. Sun, *Sci China Chem* 54 (2011) 898–910.
5. H. Zhao, Q. Li, L. Sun, *Sci China Chem* 54 (2011) 898–910.
6. T.J.B. Holland, S.A.T. Redfern, Miner. Mag. 61 (1997) 65-67.
7. M. Medarde, J. Rodriguez-Carvagal, M. Vallet-Regi, J. M. Gonzalez- Calbet, J. Alonso, Phys Rev B: Condens Matter 49 (1994) 8591–8599.
8. M. Nishijima, Y. Takeda, N. Inanishi, O. Yamamoto, R. Kanno, FuntaiOyobiFunmatsu Yakin 38 (1991) 224–228.
9. R.D. Shannon, Acta. Crys., A32 (1976) 751-767.
10. A.P. Khandale, S.S. Bhoga, J. Power Sources, 195 (2010) 7974-7982.
11. V.I. Voronin, A.E. Kar'kin, B.N. Goshchitski, Phys. Solid State 40 (2) (1998) 157-162.
12. A. P. Khandale, J. D. Punde, S. S. Bhoga, J Solid State Electrochem (2013) 17:617–626.

13. J. D. Punde, A. P. Khandale, S. S. Bhoga, Indian Journal of Pure & Applied Physics, Vol. 51, May 2013, pp.376-380.
14. Xiaomao Yang, Laitao Luo, Hua Zhong, Applied Catalysis A: General 272 (2004) 299–303.
15. H. Lou, J. Liu, X. Liu, F. Ma, J. Chin. Rare Earth Soc. 19 (2001) 324.
16. H. Zhong, R. Zeng, J. Serb. Chem. Soc. 71 (10) (2006) 1049–1059.
17. E. Bohem, J.M. Basat, M.C. Steil, P. Dordor, F. Mauvy, J.C. Grenier, Solid State Sciences 5 (2003) 973-981.
18. V.V. Vashook, I.I. Yushkeivich, L.V. Kokhonovsky, L.V. Makhonovsky, L.V. Makhanch, S.P. Tolochko, I.F. Kononyuk, H. Ullmann, H. Altenburg, Solid State Ionics 119 (1999) 23-30.